

SUPPORTING INFORMATION:

Plasmonic Zero Mode Waveguide for highly confined and enhanced fluorescence emission

Paolo Ponzellini¹‡, Xavier Zambrana-Puyalto¹‡, Nicolò Maccaferri¹, Luca Lanza¹, Francesco De Angelis¹ and Denis Garoli¹*

¹ Istituto Italiano di Tecnologia, via Morego 30, I-16163, Genova, Italy.

‡These authors contributed equally to this work

* Corresponding author: Dr. Denis Garoli, denis.garoli@iit.it

Ag-Al nanoslots, simulations.

We have simulated the near field response of the Ag-Al nanoslot at the experimental wavelength of 676 nm. This is shown in Fig. S1. The simulation has been performed with a plane wave excitation and a polarization parallel to the minor axis of the slot. The results of the simulations resemble those for the Au-Al case, with a strong field enhancement at the bottom of the nanoslot.

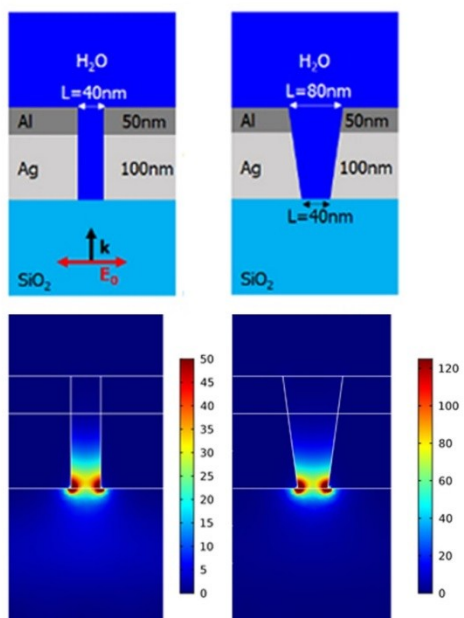


Figure S1. Sketch of a section of the ideal and fabricated rectangular Ag-Al (top panels) nanoslot. In the bottom panels the near field maps for ideal and experimental structures are reported.

The simulated broadband behaviour of the Ag-Al nanoslot is depicted in Fig. S2. Similarly to the Au-Al nanoslot case, the experimental-flared shape induces a red-shift with respect to the ideal shape. Moreover, we observe that the near-field intensity spectra of both the ideal and the experimental shape are blue-shifted with respect to the Au-Al nanoslot. Here the maximum of the average field enhancement is quite higher than that of the Au-Al nanoslot, but it occurs at a wavelength that is far away with respect to our excitation wavelength.

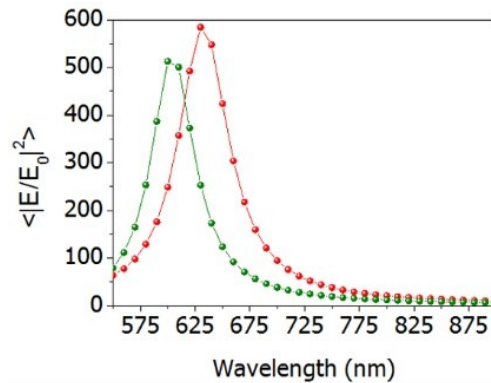


Figure S2. Calculated field enhancements, averaged on the glass/water interface at the bottom of the Ag-Al nanoslot for the rectangular-ideal (green) and flared-fabricated (red) shapes.

1. Ag-Al nanoslots, fabrication

Ag-Al samples have been fabricated similarly to the Au-Al ones (see methods). The only discrepancy regards the deposition rates of the different materials. Silver has been evaporated (instead of gold) at the rate of 1 Å/s, followed by a 50 nm aluminum layer evaporated at 1,5 Å/s. Next, we show a cross section of the milled

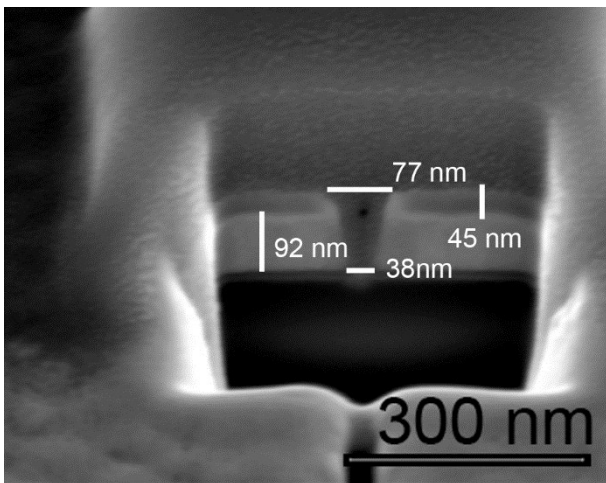


Figure S3. SEM cross section images of the silver-Aluminum nanoslot. A 90 nm silver layer and a 45 nm aluminum layer are visible as well as the platinum layer above.

Ag-Al structures in Fig. S3. The milled Ag-Al samples have undergone an oxygen plasma in order to make the surface hydrophilic. Once unloaded from the evaporator chamber, the samples have been measured within few hours, to reduce the oxidation. Unfortunately, the Ag-Al samples were unstable when they got in

contact with the fluorophore solution. As shown in Fig. S4, they started delaminating after few minutes, thus making it impossible for us to measure their fluorescence response.

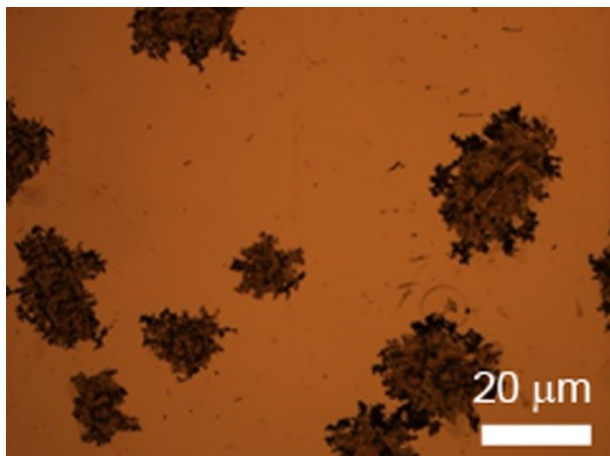


Figure S4. Delaminated Ag-Al samples. Bright field images.

Alternatively, we thought of doing the fluorescence experiment in ethanol, instead of in water. Ethanol has got a smaller surface tension, with respect to water. Therefore, the ethanol-fluorophore solution can enter the nanoslots without the need of an oxygen plasma treatment. In this way, we could avoid the oxidizing effect deriving from both the contact with water and the plasma treatment. Indeed, the Ag-Al samples were more stable in ethanol, but we did not manage to gather good data due to the high evaporation rate of ethanol.

2. FCS measurements on parametric Au-Al nanoslots

We have fabricated a parametric sample with different Au-Al nanoslots. Each nanoslot is characterized by the FIB software parameters that have been used to fabricate the slots: (x,y,z) . x - y are related to the transverse section of the antenna, and z to its depth. For every (x,y,z) set of parameters, we have fabricated nine slots. We have performed FCS measurements at least on two slots from each (x,y,z) set. In Fig. S5, we show representative fluorescence time traces for different slots. Then, in Fig. S6, we show their respective autocorrelation functions. All the measurements have been carried out with Alexa Fluor 680 at a concentration of 34 μ M. Using this data, we have computed the FE for each slot. These are displayed in Fig. 5 of the main article. The time traces and the autocorrelation function of the best performing slot in Fig. 5 have not been included here, as they are reported in the main body of the manuscript.

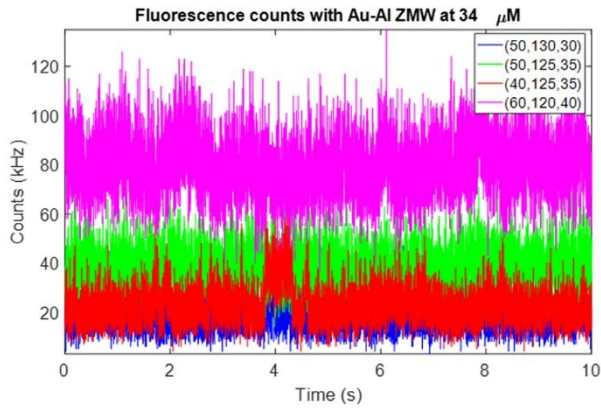


Figure S5. Fluorescence time traces with different Au-Al nanoslots. Each nanoslot is characterized by the FIB parameters that have been used to fabricate the slots. An Alexa Fluor 680 at a concentration of $34\mu\text{M}$ has been used for the measurements.

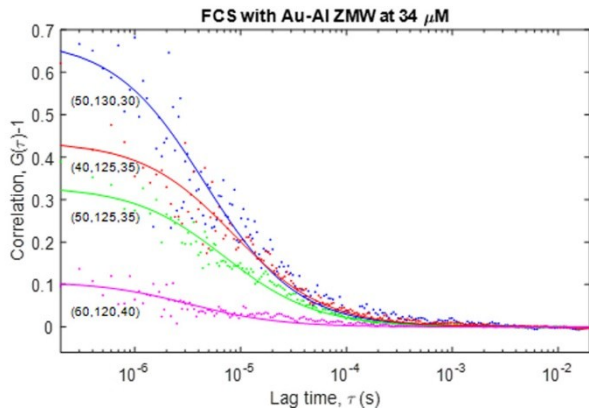


Figure S6. FCS correlation function (dots, raw data; lines, numerical fits) associated to the fluorescence time traces shown in Fig. S5. Each nanoslot is characterized by the FIB parameters that have been used to fabricate the slots. An Alexa Fluor 680 at a concentration of $34\mu\text{M}$ has been used for the measurements.

3. Simulations on Gaussian beam illumination

As discussed in the main text the comparison between the electromagnetic field confinement that can be obtained in the case of plane wave and Gaussian beam illumination has been considered. In Fig. S7 we report the results of the simulations taking into consideration different beam waists. As can be observed a significant effects is present and become negligible increasing the beam waist.

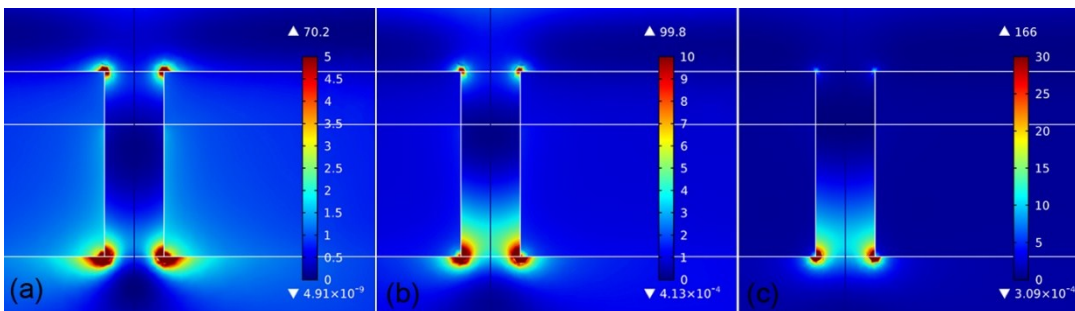


Figure S7. FEM simulation of Au/Al nanoslot. (a) Gaussian beam illumination (beam waist 500 nm); (b) Gaussian beam illumination (beam waist 1500 nm); (c) Gaussian beam illumination (beam waist 3000 nm). In all the case the color bars are set in order to make a more clear visualization of the fields.

4. Effect of the Ti adhesion layer on the field enhancement

As discussed in the main text the presence of 3 nm thick Titanium layer between glass and Gold induces an effect on the theoretical enhancement that can be achieved. In Fig. S8 the mean field intensities in the case of ideal structure and experimental structure comprising Ti are shown.

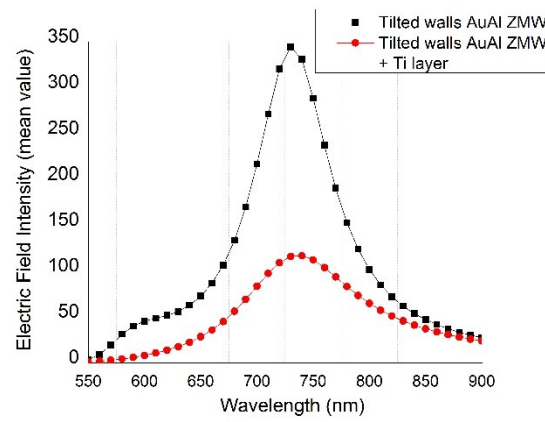


Figure S8. FEM simulation of Au/Al nanoslot with and without 3nm thick Ti adhesion layer at the glass/gold interface.